

# Oxygen Extraction Mapping from Susceptibility Difference Measurements : Comparison of Data Evaluation Strategies in a Phantom

A. Bongers<sup>1</sup>, L. R. Schad<sup>1</sup>

<sup>1</sup>Department of Medical Physics in Radiology, Deutsches Krebsforschungszentrum, Heidelberg, Germany

## Introduction:

Oxygen supply is an important factor for tissue viability. One approach to obtain information about oxygenation status is to map oxygen extraction fraction from blood (OEF) by measuring susceptibility differences between venous vessels and surrounding tissue [1]. Such susceptibility difference maps ( $\Delta\chi$ ) can be calculated from measurements of volume fraction ( $\lambda$ ) and reversible relaxation rate ( $R_2'$ ), when a model of tissue structure is assumed [2]. In this work different data evaluation strategies are investigated to obtain  $R_2'$  and  $\lambda$  from measurements with combined spin-echo/gradient-echo sequences and hence to calculate maps of susceptibility difference.

## Methods:

A custom-built phantom was used for the measurements which resembles the tissue properties of statistically distributed capillaries in a homogeneous medium as required by the model used for data evaluation (see below). The phantom consisted of 4 compartments containing randomly coiled nylon strings with radii ( $r_c=32\mu\text{m}$ ,  $50\mu\text{m}$ ,  $80\mu\text{m}$ ,  $120\mu\text{m}$ ) and a relative volume fraction of  $\lambda=5\%$  in a NiSO<sub>4</sub> solution. On a 1.5T whole body scanner (Siemens Symphony, Erlangen) a multi gradient-echo/spin-echo sequence was used to acquire 25 gradient echo images with an echo spacing of  $\Delta TE=4\text{ms}$ . The images were sampled symmetrically around a spin echo occurring at  $TE_{SE} = 118\text{ms}$ . Other sequence parameters were: 1.GE:  $TE_{GE1}=70\text{ms}$ , RO-bandwidth=500Hz, TR=1000ms, FOV=200x200mm, Matrix=128x128,  $\Delta x=\Delta y=1.6\text{mm}$ ,  $\Delta z=8\text{mm}$ . From the echo-images parameter-maps of  $\lambda$  and  $R_2'$  were calculated using the theory developed by Yablonskiy [2]. To correct for the influence of macroscopic field variations a quadratic model was fitted to the data as suggested in [3]. In the longterm-regime (i.e.  $|t-TE_{SE}|\geq 20\text{ms}$ ) the tissue model predicts the following signal-timecourse before and after the spin-echo, with the rate constants  $R_2'^{up}$  and  $R_2'^{down}$ , respectively (quadratic terms for macroscopic field correction are omitted in the equations):

$$S_{long}^{up}(t) = S_{SE} \cdot \exp(\lambda) \cdot \exp(-R_2'^{up} \cdot (t - TE)) \quad , \quad S_{long}^{down}(t) = S_{SE} \cdot \exp(\lambda) \cdot \exp(-R_2'^{down} \cdot (t - TE)) \quad (1)$$

To determine susceptibility maps for the phantom two different fitting strategies were compared.

In the *first method* [3] both signal equations (1) are fitted independently to the echo train before and after the spin-echo and  $R_2'$  and  $\lambda$  are calculated in the following way:

$$\text{Method 1: } \left\| \ln(S(TE_i - TE_{SE})) - (\lambda_{up,down} - R_2'^{up,down} \cdot (TE_i - TE_{SE}) - c(TE_i - TE_{SE})^2) \right\|_{\chi^2} \rightarrow \min \quad \Rightarrow \quad \begin{aligned} \lambda &= \frac{1}{2}(\lambda_{up} + \lambda_{down}) - \ln(S_{SE}) \\ R_2' &= \frac{1}{2}(R_2'^{down} - R_2'^{up}) \end{aligned}$$

In the *second method* the signal equations (1) are rewritten in a more compact way using the relationships  $R_2'^{up} = 1/2(R_2' - R_2')$  and  $R_2'^{down} = 1/2(R_2' + R_2')$ . From this the parameters  $R_2'$ ,  $R_2'$  and  $\lambda$  can be determined directly in a 3-parameter fit:

$$\text{Method 2: } \left\| \ln(S(TE_i - TE_{SE})/S_{SE}) - (\lambda - R_2'(TE_i - TE_{SE}) - R_2'|TE_i - TE_{SE}| - c(TE_i - TE_{SE})^2) \right\|_{\chi^2} \rightarrow \min$$

For both methods  $\Delta\chi$ -maps were calculated from the  $R_2'$ - and  $\lambda$ -maps using  $\Delta\chi = \left(\frac{4}{3}\pi \cdot \lambda \cdot \gamma \cdot B_0\right)^{-1} \cdot R_2'$ .

## Results :

In Fig 1a the log-timecourse of an echo-train for one pixel within a phantom compartment is shown. The occurrence of the spin-echo is highlighted by the vertical line in the centre. The fitting curves for methods 1 and 2 are plotted as dotted and compact line, respectively. The independent fit curves do not intersect the  $t=0$  axis at the same point which shows the poorer stability of the extrapolation and hence of the determination of  $\lambda$ . Method 2 shows a better performance. In Fig 1b and 1c the calculated  $\Delta\chi$ -maps are shown in a linear colour-scale. The 4 phantom compartments are depicted in red/yellow. The compartments show quite homogeneous susceptibility differences but also some (dark coloured) noise pixels which are due to large parameter uncertainties. In these pixels the statistical uncertainty becomes larger than the determined value. As should be expected, the homogenous areas outside the compartments show mostly noise – no susceptibility difference is measured. Comparing both  $\Delta\chi$ -maps the superior stability of the combined fit to the data (method 2) becomes obvious. (See e.g. the third phantom compartment (white arrow)).

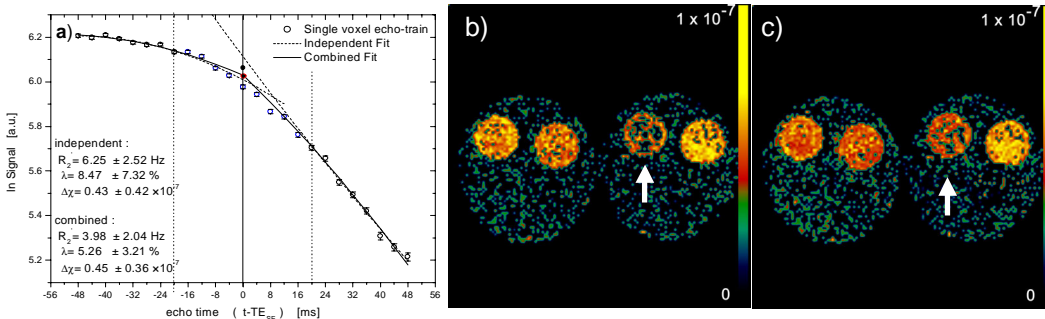


**Fig.1:** a) Typical timecourse from the GE/SE- measurements within a compartment with both fitting functions (dotted line = method 1, compact line = method 2),

b)  $\Delta\chi$ -map of the phantom calculated with method 1, c)  $\Delta\chi$ -map of the phantom calculated with method 2

## Discussion:

In this work two data evaluation methods for the calculation of susceptibility difference maps are compared. It is shown that rewriting the theoretical signal-timecourse in a compact form and fitting the whole echo-train with one function results in considerably better stability of the calculated  $\Delta\chi$ -maps than direct, independent fitting. This has two reasons: First, for method 2 a lower number of parameters is needed to fit the data and secondly, method 2 does not need an extrapolation for the determination of  $\lambda$ . This causes a marked advantage of method 2 over method 1 - especially when a correction for field inhomogeneities using quadratic fitting is applied.

## References:

- [1] H. An, W. Lin, Cerebral oxygen extraction fraction and cerebral venous blood volume measurements using MRI: Effects of magnetic field variation. *Magn Reson Med* **47**, 958-966 (2002)
- [2] D.A. Yablonskiy, E.M. Haacke, Theory of NMR signal behavior in magnetically inhomogeneous tissues: The static dephasing regime. *Magn Reson Med* **32**, 749-63 (1994)
- [3] D.A. Yablonskiy, Quantitation of intrinsic magnetic susceptibility-related effects in a tissue matrix. *Magn Reson Med* **39**, 419-428 (1998)